Testing color evaporation in photon-photon production of J/ψ at CERN LEP II

O. J. P. Éboli,[1,*] E. M. Gregores,[2,†] and J. K. Mizukoshi[1,‡]
[1]*Instituto de Física, Universidade de São Paulo, São Paulo, SP, Brazil*
[2]*Instituto de Física Teórica, Universidade Estadual Paulista, São Paulo, SP, Brazil*
(Received 18 August 2003; published 11 November 2003)

The DELPHI Collaboration has recently reported the measurement of J/ψ production in photon-photon collisions at CERN LEP II. These newly available data provide additional proof of the importance of colored $c\bar{c}$ pairs for the production of charmonium, because these data can be explained only by considering resolved photon processes. We show here that the inclusion of color octet contributions to J/ψ production in the framework of the color evaporation model is able to reproduce these data. In particular, the transverse-momentum distribution of the J/ψ mesons is well described by this model.

DOI: 10.1103/PhysRevD.68.094009 PACS number(s): 13.60.Le, 14.40.Gx

I. INTRODUCTION

The DELPHI Collaboration recently released preliminary measurements of the transverse-momentum spectrum of J/ψ mesons produced in $\gamma\gamma$ collisions at the CERN e^+e^- collider LEP [1,2]. These new data allow further tests of models for charmonium production. We show here that the color evaporation model (CEM) reproduces these new results using the same single nonperturbative parameter that has been obtained from previous analysis of charmonium photo- and hadroproduction. These newly available data provide additional proof of the importance of colored $c\bar{c}$ pairs for the production of charmonium, as the data in this region can be explained only by considering resolved photon processes, which form colored $c\bar{c}$ pairs in the leading order. The CEM for charmonium production incorporates these colored pairs into the total yield of charmonium in a very simple and economical way.

The Fermilab Tevatron data [3,4] on charmonium production at high p_T have changed the way we understand charmonium production. The presently successful models are based on two key considerations: (i) quarkonium production is a two-step process in which a heavy quark pair is produced first, followed by the nonperturbative formation of the asymptotic states, and (ii) color octet as well as singlet $c\bar{c}$ states contribute to the production of charmonia. These features are incorporated in the nonrelativistic QCD (NRQCD) factorization approach [5,6], the color evaporation model [7–9] and the soft color interaction model [10].

The color evaporation model simply states that charmonium production is described by the same dynamics as $D\bar{D}$ production, i.e., by the formation of a $c\bar{c}$ pair in any color configuration. Rather than imposing that the $c\bar{c}$ pair is in a color singlet state in the short distance perturbative processes, it is argued that the appearance of color singlet asymptotic states solely depends on the outcome of nonperturbative large distance fluctuations of quarks and gluons. These large distance fluctuations are considered to be complex enough for the occupation of different color states to approximately respect statistical counting. In fact, it is indeed hard to imagine that a color singlet state formed at a range m_ψ^{-1} would survive to form a ψ at a range Λ_{QCD}^{-1}. Although far more restrictive than other proposals, the CEM successfully accommodates all features of charmonium production [11–13].

The CEM predicts that the sum of the production cross sections of all quarkonium and open charm states is described by

$$\sigma_{\text{quarkonium}} = \frac{1}{9}\int_{2m_c}^{2m_D} dM_{c\bar{c}} \frac{d\sigma_{c\bar{c}}}{dM_{c\bar{c}}} \tag{1}$$

and

$$\sigma_{\text{open}} = \frac{8}{9}\int_{2m_c}^{2m_D} dM_{c\bar{c}} \frac{d\sigma_{c\bar{c}}}{dM_{c\bar{c}}} + \int_{2m_D} dM_{c\bar{c}} \frac{d\sigma_{c\bar{c}}}{dM_{c\bar{c}}}, \tag{2}$$

where $M_{c\bar{c}}$ is the invariant mass of the $c\bar{c}$ pair. The factor 1/9 stands for the probability that a pair of charm quarks formed at a typical time scale $1/M_\psi$ ends up as a color singlet state after exchanging an uncountable number of soft gluons with the reaction remnants; for further details see [7]. One attractive feature of this model is the relation between the production of charmonium and open charm, which allows us to use the open charm data to normalize the perturbative QCD calculation, and consequently to constrain the CEM predictions.

Up to this point, the model has no free parameter in addition to the usual QCD ones. In order to predict the production rate of a particular charmonium state, let us say a J/ψ meson, we must also know the fraction ρ_ψ of produced quarkonium states that materialize as this state (J/ψ),

$$\sigma_\psi = \rho_\psi \sigma_{\text{quarkonium}}. \tag{3}$$

In its simplest version, the CEM assumes that ρ_ψ is energy and process independent, which is in agreement with the low energy measurements [14,15]. Notice that ρ_ψ is the only free parameter of the CEM, making this a very restrictive frame-

*Electronic address: eboli@fma.if.usp.br
†Electronic address: gregores@ift.unesp.br
‡Electronic address: mizuka@fma.if.usp.br

work. From charmonium photoproduction, we determined that $\rho_\psi = 0.43$–0.5 [8], a value that can be accounted for by statistical counting of final states [10]: the fraction of a given quarkonium state X with angular momentum J_X can be written as $\rho_X = \Gamma_X / \Sigma_Y \Gamma_Y$ with $\Gamma_X = (2J_X+1)/n_X$. Notice that a suppression factor for radially excited states with principal quantum number n_x has been introduced; for further details see Ref. [10]. The fact that all ψ production data are described in terms of this single parameter, fixed by J/ψ photoproduction, leads to parameter-free predictions for the Z boson decay rate into ψ [16], and to charmonium production cross sections at the Tevatron [17] and the DESY ep collider HERA [18,19], as well as in neutrino initiated reactions [20].

II. RESULTS

The differential cross section for the inclusive process $e^+e^- \to e^+e^- \gamma\gamma \to J/\psi X$ is

$$\frac{d^2\sigma}{dp_T^2} = \sum_{A,B} \int\int\int\int dy^+ dy^- dx_A dx_B f_{\gamma/e^+}(y^+) \times f_{\gamma/e^-}(y^-) F_{A/\gamma}(x_A) F_{B/\gamma}(x_B) \frac{d^2\hat{\sigma}(AB \to \psi Y)}{dp_T^2}, \tag{4}$$

where $f_{\gamma/e^\pm}$ is the bremsstrahlung photon distribution from an electron or positron. We denoted the parton distribution function of the photon by $F_{A[B]/\gamma}(x_{A[B]})$, where $x_{A[B]}$ is the fraction of the photon momentum carried by the parton $A[B]$. For direct photon interactions ($A[B] \equiv \gamma$), we have $F_{A[B]/\gamma}(x_{A[B]}) = \delta(x_{A[B]} - 1)$. We considered an average electron-positron center-of-mass energy $2E_e = 197$ GeV. We also applied the experimental J/ψ rapidity cut $-2 < \eta_\psi < 2$, and imposed that the $\gamma\gamma$ center-of-mass energy satisfies $W_{\gamma\gamma} < 35$ GeV, where $W_{\gamma\gamma} = 2E_e\sqrt{y^+y^-}$.

In our calculation, we employed the Weizäcker-Williams approximation for the photon distribution,

TABLE I. Subprocesses contributing to J/ψ production in $\gamma\gamma$ collisions. Here q stands for the light quark flavors u,d,s.

Direct	Once resolved	Twice resolved
$\gamma\gamma \to c\bar{c}g$	$\gamma q(\bar{q}) \to c\bar{c}q(\bar{q})$	$q\bar{q} \to c\bar{c}g$
	$\gamma g \to c\bar{c}g$	$gq(\bar{q}) \to c\bar{c}q(\bar{q})$
		$gg \to c\bar{c}g$

$$f_{\gamma/e^\pm}(y) = \frac{\alpha_{e.m.}}{2\pi}\left[\frac{1+(1-y)^2}{y}\log\left(\frac{Q^2_{max}}{Q^2_{min}}\right) + 2m_e^2 y\left(\frac{1}{Q^2_{max}} - \frac{1}{Q^2_{min}}\right)\right], \tag{5}$$

with $Q^2_{min} = m_e^2 y^2/(1-y)$, and $Q^2_{max} = (E_e\theta)^2(1-y) + Q^2_{min}$. Here, the fraction of the parent $e^\pm$ energy (E_e) carried by the photons is $y(=E_\gamma/E_e)$, and θ is the angular cut that guarantees that the photons are real. We used $\theta = 0.032$ rad, as determined by the experiment.

The inclusive subprocess cross section $\hat{\sigma}(AB \to \psi Y)$ was calculated using the CEM; see Eqs. (1) and (3). The partonic subprocesses contributing to J/ψ production are depicted in Table I. Notice that both direct and resolved photons contribute to charmonium production in the CEM. We evaluated numerically the tree level helicity amplitudes of the subprocesses displayed in Table I using the MADGRAPH [21] and HELAS [22] packages. The adaptive Monte Carlo program VEGAS [23] was employed to perform the phase space integration.

In the framework of the CEM, the evaluation of the photon-photon production cross section contains only the free parameters appearing in the perturbative QCD calculation of the subprocesses presented in Table I, since the CEM free parameter ρ_ψ can be fixed at the value extracted from the photoproduction of J/ψ, i.e., $\rho_\psi = 0.5$ [8]. We used the leading order GRV-G [24] and GRS-G [25] parton density functions as provided by the CERN PDFLIB package with the partonic subprocess center-of-mass energy as the factoriza-

TABLE II. Cross sections for direct, once resolved, and twice resolved production processes for $p_T^2 > 0.25$ GeV^2 using different sets of parton distribution functions (PDF), charm masses, and renormalization scales $\mu_R = \xi\sqrt{m_c^2 + \beta p_T^2}$.

	Parameters			Cross sections (pb)			
PDF	m_c	ξ	β	Direct	Once resolved	Twice resolved	Total
GRV-G	1.3	1.0	0	1.72	13.3	1.00	16.1
GRS-G	1.3	1.0	0	1.72	13.0	0.94	15.7
GRS-G	1.2	1.0	0	2.75	21.8	1.73	26.3
GRS-G	1.4	1.0	0	1.02	7.5	0.51	9.07
GRS-G	1.3	0.5	0	3.26	46.8	6.42	56.4
GRS-G	1.3	0.5	1	2.42	28.4	3.15	34.0
GRS-G	1.3	1.0	1	1.44	9.65	0.61	11.7
GRS-G	1.3	2.0	0	1.17	5.99	0.29	7.45
GRS-G	1.3	2.0	1	1.03	4.84	0.22	6.08

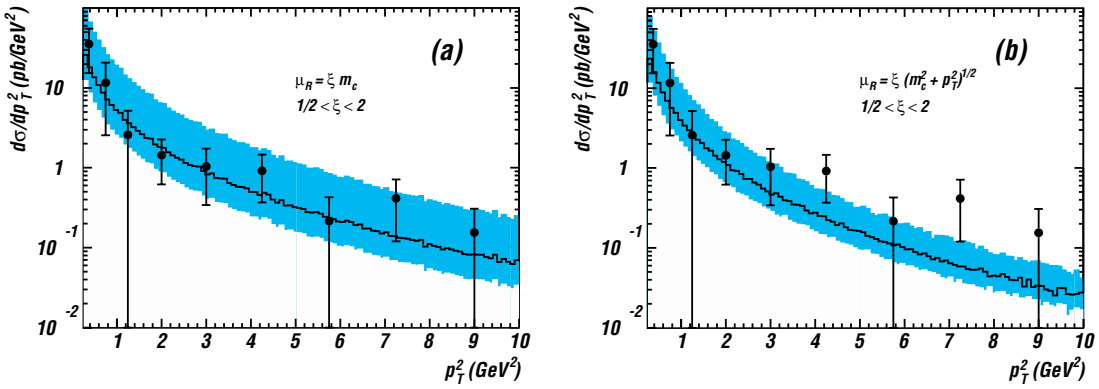

FIG. 1. Uncertainty in the p_T^2 differential cross section originating from different choices of the renormalization scale μ_R. In (a) we chose $\mu_R = \xi m_c$ while in (b) $\mu_R = \xi\sqrt{m_c^2 + p_T^2}$. The shaded band was obtained by varying $1/2 < \xi < 2$ and the solid line stands for $\xi = 1$. We fixed $m_c = 1.3$ GeV, and used the GRS-G parton density function in both figures.

tion scale $\mu_F = \sqrt{\hat{s}}$. We verified that our predictions do not vary significantly ($\lesssim 10\%$) for other choices of the factorization scales, e.g., $\mu_F = \frac{1}{2}\sqrt{\hat{s}}$, $\mu_F = 2\sqrt{\hat{s}}$, or $\mu_F = \mu_R$. We also verified that the results are very similar for the GRV-G and GRS-G parton distributions (see Table II). The strong coupling constant was evolved in leading order considering four active flavors and $\Lambda_{QCD}^{(4)} = 300$ MeV, while the charm quark mass was varied between 1.2 and 1.4 GeV.

In order to access the theoretical uncertainties in the lowest order CEM calculations, we analyzed the predicted J/ψ transverse-momentum spectrum for different choices of the renormalization scale (μ_R). We present in Fig. 1(a) the predicted p_T^2 spectrum obtained for $\mu_R = \xi m_c$ with $\frac{1}{2} < \xi < 2$ and $m_c = 1.3$ GeV, as well as the DELPHI experimental results [1,27]. We can see from this figure that the CEM describes well the shape of the distribution, despite the large uncertainty in the absolute value of the differential cross section. Notice that we are only changing a global factor (α_S) for this choice of μ_R when we vary ξ. Figure 1(b) displays the p_T^2 spectrum for $\mu_R = \xi\sqrt{m_c^2 + p_T^2}$ with $\frac{1}{2} < \xi < 2$ and $m_c = 1.3$ GeV. For this choice of μ_R the uncertainties in the p_T^2 distribution are smaller than for the previous choice of μ_R. However, the shape of the p_T^2 spectrum changes and the CEM prediction seems to diminish faster than the data at large p_T^2.

In Fig. 2 we display the contributions to the J/ψ p_T^2 spectrum arising from direct, once resolved, and twice resolved processes. These distributions were obtained using the GRS-G photon parton densities, $\mu_R = m_c$, and $m_c = 1.3$ GeV. As we can see, the once resolved processes are responsible for the majority of the events ($\simeq 85\%$), while direct and twice resolved processes account for less than 15% of the total cross section. The most important process is $\gamma g \to c\bar{c}g$. We also present in this figure the uncertainties associated with the charm quark mass; the shaded band represents the sum of all contributions taking $m_c = 1.3 \pm 0.1$ GeV. Notice that the largest uncertainties in the CEM prediction originate from the choice of the renormalization scale. This is quite as expected since we are performing our calculation in lowest order perturbative QCD. In fact, the charmonium production in $\gamma\gamma$ collisions is dominated by once resolved photon processes; therefore it is similar to the photoproduction of charm quark pairs. In this case, it is well known that the K factor is of the order of 2–3 [26], and consequently we can anticipate that the next-to-leading order corrections to our results should be of this magnitude. We summarize our results for the total cross section in Table II.

In order to further compare our results with the recently published DELPHI results [2,27], we evaluated the dependence of the total J/ψ yield on the minimum transverse momentum for $\sqrt{s} = 197$ GeV. The result is presented in Fig. 3(a). As can be seen from this figure, the choice of QCD parameters we used in this analysis provides a very good description of the existing data, reinforcing our confidence in the predictive power of the color evaporation model. Figure 3(b) displays the CEM predictions for the J/ψ production cross section as a function of the e^+e^- center-of-mass energy ($\sqrt{s}$). Here we assumed that $p_T^2 > 0.25$ GeV^2, $\mu_R = m_c$ with $m_c = 1.3 \pm 0.1$ GeV, and we used the GRS-G set of parton distribution functions. As expected, the total cross section grows with the center-of-mass energy due to the increase in

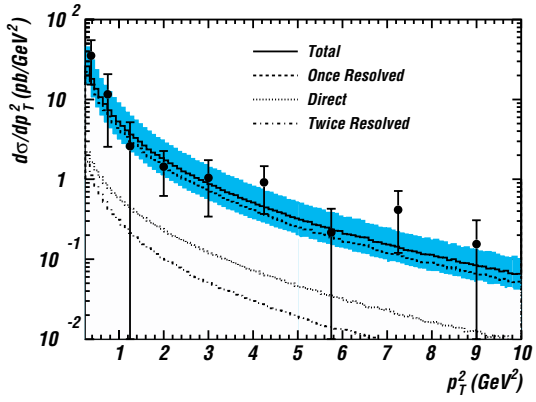

FIG. 2. Differential cross section as a function of the squared transverse momentum of the J/ψ. The shaded band shows the theoretical prediction obtained by varying the charm mass ($m_c = 1.3 \pm 0.1$ GeV). We explicitly show the direct, once resolved, and twice resolved contributions as well as the total cross section for $m_c = 1.3$ GeV.

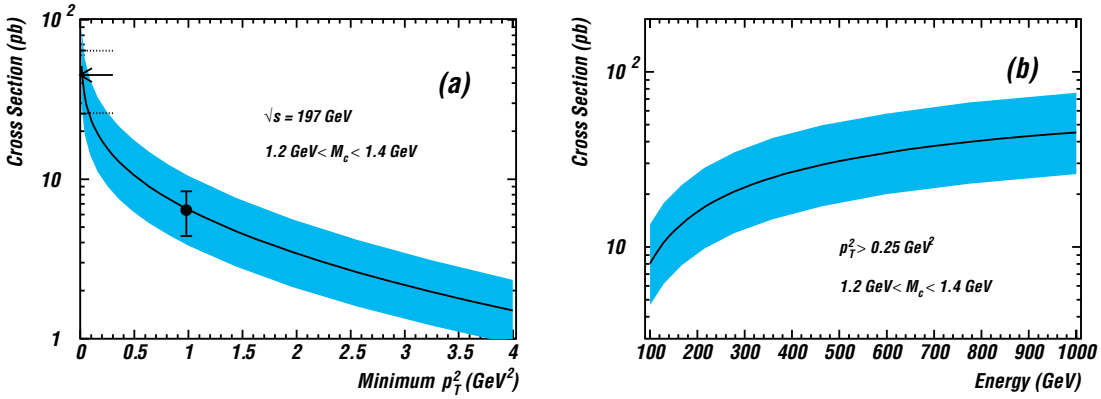

FIG. 3. Total cross section as function of the minimum squared transverse momentum (a) and the e^+e^- center-of-mass energy (b). In (a) the arrow stands for the DELPHI measured total cross section while the dotted lines indicate the experimental error of this quantity. We varied the charm quark mass as $m_c = 1.3 \pm 0.1$ GeV to estimate the theoretical uncertainties. We used $\sqrt{s} = 197$ GeV for the minimum transverse-momentum dependence (a) and imposed $p_T^2 > 0.25$ GeV^2 for the center-of-mass energy dependence (b). The remaining parameters are the same as for Fig. 2. In both figures, the solid line represents $m_c = 1.3$ GeV.

the photon-photon luminosity. We verified that contributions of direct, once resolved, and twice resolved, processes are in the same proportion as for the results presented for $\sqrt{s} = 197$ GeV; see Fig. 2. Taking into account the planned luminosity of the future e^+e^- colliders, we can easily foresee that it will be possible to extract very precise data on the photon-photon charmonium production in these machines.

III. CONCLUSION

In this paper we showed that the color evaporation model for quarkonium production correctly describes DELPHI data on J/ψ via photon-photon collisions. Because of the rather large uncertainties in the data, it is not possible to use them to discriminate between the different proposed mechanisms for charmonium production. As far as the DELPHI data are considered, the NRQCD [27] and CEM frameworks present equivalent results.

Considering that the CEM is also successful in describing the photo- and hadroproduction of charmonium, we conclude that this model gives a robust and simple parameterization of all charmonium physics. Moreover, $\gamma\gamma$ reactions provide a clear proof of the importance of colored $c\bar{c}$ pairs in the production of charmonium, since the data on this reaction can be explained only by considering resolved photon processes, which lead to colored $c\bar{c}$ pairs.

ACKNOWLEDGMENTS

This research was supported in part by Fundação de Amparo à Pesquisa do Estado de São Paulo (FAPESP), by Conselho Nacional de Desenvolvimento Científico e Tecnológico (CNPq), and by Programa de Apoio a Núcleos de Excelência (PRONEX).

[1] S. Todorova-Nova, in Proceedings of the 31st International Symposium on Multiparticle Dynamics (ISMD 2001), Datong, China, 2001, edited by B. Yuting, Y. Meiling, and W. Yuanfang, eConf C010901, 2001.
[2] DELPHI Collaboration, J. Abdallah *et al.*, Phys. Lett. B **565**, 76 (2003).
[3] CDF Collaboration, F. Abe *et al.*, Phys. Rev. Lett. **69**, 3704 (1992); **79**, 572 (1997); **79**, 578 (1997).
[4] DØ Collaboration, S. Abachi *et al.*, Phys. Lett. B **370**, 239 (1996).
[5] G.T. Bodwin, E. Braaten, and G.P. Lepage, Phys. Rev. D **51**, 1125 (1995); **55**, 5853(E) (1997).
[6] E. Braaten, S. Fleming, and T.C. Yuan, Annu. Rev. Nucl. Part. Sci. **46**, 197 (1996).
[7] J.F. Amundson, O.J.P. Éboli, E.M. Gregores, and F. Halzen, Phys. Lett. B **372**, 127 (1996).
[8] J.F. Amundson, O.J.P. Éboli, E.M. Gregores, and F. Halzen, Phys. Lett. B **390**, 323 (1997).
[9] O.J.P. Éboli, E.M. Gregores, and F. Halzen, in *Proceedings of the 26th International Symposium on Multiparticle Dynamics (ISMD 96)*, Faro, Portugal, 1996, edited by J. Dias de Deus *et al.* (World Scientific, Singapore, 1997).
[10] A. Edin, G. Ingelman, and J. Rathsman, Phys. Rev. D **56**, 7317 (1997).
[11] C.B. Mariotto, M.B. Gay Ducati, and G. Ingelman, Eur. Phys. J. C **23**, 527 (2002).
[12] M. Kramer, Prog. Part. Nucl. Phys. **47**, 141 (2001).
[13] G.A. Schuler and R. Vogt, Phys. Lett. B **387**, 181 (1996).
[14] R. Gavai, D. Kharzeev, H. Satz, G.A. Schuler, K. Sridhar, and R. Vogt, Int. J. Mod. Phys. A **10**, 3043 (1995).
[15] G.A. Schuler, hep-ph/9403387.
[16] O.J.P. Éboli, E.M. Gregores, and F. Halzen, Phys. Lett. B **395**, 113 (1997).
[17] O.J.P. Éboli, E.M. Gregores, and F. Halzen, Phys. Rev. D **60**, 117501 (1999).

[18] O.J.P. Éboli, E.M. Gregores, and F. Halzen, Phys. Lett. B **451**, 241 (1999).
[19] O.J.P. Éboli, E.M. Gregores, and F. Halzen, Phys. Rev. D **67**, 054002 (2003).
[20] O.J.P. Éboli, E.M. Gregores, and F. Halzen, Phys. Rev. D **64**, 093015 (2001).
[21] T. Stelzer and W.F. Long, Comput. Phys. Commun. **81**, 357 (1994).
[22] H. Murayama, I. Watanabe, and K. Hagiwara, Report No. KEK-91-11.
[23] G.P. Lepage, Report No. CLNS-80/447.
[24] M. Gluck, E. Reya, and A. Vogt, Phys. Rev. D **46**, 1973 (1992); **45**, 3986 (1992).
[25] M. Gluck, E. Reya, and M. Stratmann, Phys. Rev. D **51**, 3220 (1995).
[26] S. Frixione, M.L. Mangano, P. Nason, and G. Ridolfi, Nucl. Phys. **B412**, 225 (1994).
[27] M. Klasen, B.A. Kniehl, L.N. Mihaila, and M. Steinhauser, Phys. Rev. Lett. **89**, 032001 (2002).